Received: 14 February 2020 | Revised: 8 June 2020 | Accepted: 8 June 2020 | Published online: 11 August 2020

DOI: 10.1002/dad2.12064

Alzheimer's & Dementia
Diagnosis, Assessment & Disease Monitoring

RESEARCH ARTICLE

# Untargeted metabolomics reveal dysregulations in sugar, methionine, and tyrosine pathways in the prodromal state of AD

**Ihab Hajjar**[1] | **Chang Liu**[2] | **Dean P. Jones**[2] | **Karan Uppal**[2]

[1] Medicine and Neurology, Department of Neurology, Emory University, Atlanta, Georgia, USA

[2] Department of Medicine, Emory University, Atlanta, Georgia, USA

**Correspondence**
Ihab Hajjar, Associate Professor of Medicine and Neurology, Department of Neurology, Emory University, 6 Executive Park, Atlanta, GA 30329, USA.
E-mail: ihabhajjar@emory.edu

## Abstract

**Introduction:** Altered metabolism may occur years before clinical manifestations of Alzheimer's disease (AD). We used untargeted metabolomics on the cerebrospinal fluid of patients with mild cognitive impairment (MCI) to uncover metabolomic derangements.

**Methods:** CSF from 92 normal controls and 93 MCI underwent untargeted metabolomics using high-resolution mass spectrometry with liquid chromatography. Partial least squares discriminant analysis was used followed by metabolite annotation and pathway enrichment analysis (PES). Significant features were correlated with disease phenotypes.

**Results:** We identified 294 features differentially expressed between the two groups and 94 were annotated. PES showed that sugar regulation (N-glycan, $P = .0007$; sialic acid, $P = .0014$; aminosugars, $P = .0042$; galactose, $P = .0054$), methionine regulation ($P = .0081$), and tyrosine metabolism ($P = .019$) pathways were differentially activated and significant features within these pathways correlated with multiple disease phenotypes.

**Conclusion:** There is a metabolic signature characterized by impairments in sugars, methionine, and tyrosine regulation in MCI. Targeting these pathways may offer new therapeutic approaches to AD.

KEYWORDS
Alzheimer's disease, cerebrospinal fluid, metabolism, mild cognitive impairment

## 1 | INTRODUCTION

Alzheimer's disease (AD) is characterized by a complex set of molecular pathways that begin decades before symptoms start.[1,2] Changes in proteins, lipids, and many other molecular networks have been described.[3,4] The overlapping and interaction of these networks can obscure the root pathogenic mechanisms when not fully accounted for in molecular or analytical methods. The level of complexity in these networks is becoming more evident as the cumulative knowledge of AD pathogenesis has increased in the last decade. Disentangling these complexities is becoming more feasible due to the significant advances in high throughput technologies[5] coupled with novel

bioinformatic tools including those developed by our team.[6] Recent examples applying the high throughput measurements of thousands of metabolites coupled with advanced bioinformatic approaches has comprehensively described molecular alterations and pathways in multiple diseases.[7-10] We apply these advances in investigating underlying metabolic changes in AD.

Metabolomic research focuses on examining metabolites, small molecules (typically <1500 Da) that are end products of multiple biological pathways and processes. The human metabolome is estimated to contain ≈150,000 or more of such metabolites and a large fraction are still unidentified.[11] Metabolomics aid in identifying downstream perturbations from the genetic and post genetic pathways reflecting a functional signature of biochemical activities that are closer to the phenotypical changes.[12] Our work uses high resolution untargeted metabolomic approaches, which can be a powerful tool in describing novel and previously unknown pathways involved in AD pathogenesis.

Brain hypometabolism has been reported in symptomatic AD as well as before the onset of cognitive symptoms.[13] Preliminary studies have suggested the existence of multiple metabolic changes in this prodromal stage.[14,15] However, many previous studies have either included small samples for cerebrospinal fluid (CSF) analyses,[16-18] used targeted approaches, or focused on plasma profiling.[16-19] In this study, we conducted a case-control untargeted high resolution metabolomic study on the CSF of a larger sample, relative to published CSF studies to date, of normal cognition (NC) and mild cognitive impairment (MCI), a prodromal state for AD. We aimed at investigating the alterations between NC and MCI in the metabolome and metabolic pathways using an established high resolution metabolomic biospecimen and data analysis pipeline. We further explored the association of these metabolic alterations with multiple disease phenotypes related to cognition, CSF amyloid beta 1-42 (A$\beta$42) and tau biomarkers, and brain magnetic resonance imaging (MRI) measures.

**HIGHLIGHTS**

- Metabolic signature is detectable in amnestic mild cognitive impairment (MCI), a prodromal state for Alzheimer's disease.
- This signature includes dysregulation in sugars, methionine, and tyrosine metabolism.
- S-adenosylmethionine is under- and S-adenosylhomocysteine is overexpressed in MCI.

**RESEARCH IN CONTEXT**

1. Systematic review: The authors searched PUBMED and Google Scholar for previous reports of metabolomics and Alzheimer's disease (AD). Search terms included: mild cognitive impairment, Alzheimer's disease "AND" metabolism, metabolomics. This search resulted in the following findings: Prior studies have either included small samples, used targeted approaches, or focused on plasma profiling. In this study, we conducted a case-control untargeted high resolution metabolomic study on the cerebrospinal fluid of a larger sample of normal cognition and mild cognitive impairment (MCI).
2. Interpretation: We discovered that multiple pathways, including pathways in sugar, methionine and homocysteine, and tyrosine metabolism were dysregulated in AD. Further, features that were significantly different between MCI and normal cognition had different patterns of association with cognitive, neuroimaging, and amyloid and tau biomarkers.
3. Future direction: These pathways offer new potential targets for AD.

## 2 | METHODS

### 2.1 | Participant description

Data for the current analysis were drawn from the baseline assessment of participants in the Brain Stress Hypertension and Aging program (B-SHARP) at Emory University. B-SHARP participants undergo baseline cognitive assessments, neuroimaging, and lumbar punctures and are subsequently enrolled clinical studies. This analysis used data from the 185 participants enrolled from March 2016 to January 2019 who had CSF obtained during their baseline evaluations. The protocol was approved by the Emory University Institutional Review Board prior to recruitment. Each participant provided a written informed consent.

The sample includes community-dwelling adults 50 years or older with NC or amnestic MCI. Potential study participants were identified either through a referral from the Goizueta Alzheimer's Disease Research Center at Emory or through strategic community partnerships with grass roots health education organizations, health fairs, advertisements, and mail out announcements. An appropriate study informant, defined as an individual who has regular contact with the participant at least once a week (in person or telephone), was also identified for each participant. The potential study participant attended a screening visit, during which they underwent cognitive testing. A study physician also performed a clinical evaluation, cognitive interview, and a lumbar puncture (LP).

### 2.2 | Cognitive diagnosis and exclusionary criteria

Amnestic MCI categorization was done using modified Peterson criteria. This modification included using the Montreal Cognitive Assessment (MoCA)[20] instead of Mini-Mental State Exam.[21] MCI criteria included subjective memory complaints, a MoCA < 26, Clinical Dementia Rating (CDR) score, memory sum of boxes=0.5,[22]

education adjusted cutoff score on Logical Memory delayed recall of the Wechsler Memory Scale,[23] and preserved Functional Assessment Questionnaire (FAQ)<=7.[24] Individuals with amnestic MCI are at high risk for progression into dementia due to AD and hence may be considered a prodromal state for AD.[25]

NC was defined as having no significant memory complaints beyond those expected for age, a MoCA score ≥26 points, a CDR score of 0 (including 0 on the Memory Box score), and preserved FAQ <=7. Participants were excluded if they had a history of stroke in the past 3 years, were unwilling or unable to undergo study procedures including MRI and LP, did not have a study informant, had a clinical diagnosis of dementia of any type, or abnormal serum thyroid stimulating hormone (>10) or B12 (<250).

## 2.3 | Cognitive assessment and biomarker measurements

Demographics (age, sex, education), anthropometrics (weight and height), medical diagnosis, and medications were collected at baseline by interview. Cognitive assessment included those described above plus Trail Making Tests (TMT Part A and B) a measure of executive function and Hopkins Verbal Learning Test (HVLT) for episodic memory. Cognitive assessment was performed by trained personnel supervised by the study neuropsychologist. After a fast of at least 6 hours, CSF samples were collected via LP using 24G Sprotte atraumatic spinal needles. Samples were collected in sterile polypropylene tubes, separated into 0.5cc aliquots, and stored at −80°C. Samples were subsequently shipped to and analyzed by the Biomarker Research Laboratory at the University of Pennsylvania (Dr. Leslie Shaw).[26] CSF biomarkers: A$\beta$, t-tau, and p-tau were measured using the multiplex with the multiplex xMAP Luminex platform (Luminex Corp, Austin, TX) with Innogenetics (INNO-BIA AlzBio3; Ghent, Belgium; for research use–only reagents) immunoassay kit–based reagents. The test–retest reliabilities are 0.98, 0.90, and 0.85 for t-tau, A$\beta$, and p-tau181p, respectively.[26]

## 2.4 | MRI brain imaging

Brain magnetic resolution imaging (MRIs) were also completed at Emory University (3.0 Tesla Trio MRI scanner, Siemens Medical Solutions, Malvern, PA). Anatomical images were acquired using high-resolution three-dimensional (3D) magnetization-prepared rapid acquisition with gradient echo (MPRAGE). Images were then digitally saved for offline processing. Hippocampal volume and other volumetric measurements were calculated using the free surfer package with manual supervision. Quality checks were performed for each scan. Left and right hippocampal volumes were obtained and combined to derive the total hippocampal volume and cortical thickness. Intracranial volume (ICV, $mm^3$) was also derived from this analysis. Volumetric measurements using free surfer has been shown to provide similar estimates to a fully manual procedure.[27] We used ICV-adjusted hippocampal volume to reflect the degree of neurodegeneration for each participant.[28]

## 2.5 | Untargeted metabolomic high-resolution metabolomics approaches and pipeline

Our metabolomic approaches used an established pipeline developed at the Clinical Biomarker Laboratory, led by Dr. Dean Jones (diagrammatic representation of this pipeline is included in Figure S1 in supporting information). High-resolution metabolomics (HRM) was completed using established methods by an analyst blinded to sample identity.[8,29] Briefly, CSF samples were prepared and analyzed in batches of 20. Prior to analysis, CSF aliquots were removed from storage at −80°C and thawed on ice. A 65 µL aliquot of CSF was then treated with 130 µL of liquid chromatography-mass spectrometry (LC-MS) grade acetonitrile, equilibrated for 30 minutes on ice and centrifuged (16.1 × g at 4°C) for 10 minutes to remove precipitated proteins. The supernatant was added to an autosampler vial and maintained at 4°C until analysis. Sample extracts were analyzed using LC and Fourier transform high-resolution mass spectrometry (Dionex Ultimate 3000, Q-Exactive HF, Thermo Scientific). For each sample, 10 µL aliquots were analyzed in triplicate using hydrophilic interaction liquid chromatography (HILIC) with electrospray ionization source operated in positive mode. This use of complementary chromatography phases and ionization polarity has been shown to improve detection of endogenous and exogenous chemicals.[30] Analyte separation was accomplished by HILIC using a 2.1 mm × 100 mm × 2.6 µm Accucore HILIC column (Thermo Scientific) and an eluent gradient (A = 2% formic acid, B= water, C= acetonitrile) consisting of an initial 1.5 minutes period of 10% A, 10% B, 80% C, followed by linear increase to 10% A, 80% B, 10% C at 6 minutes and then held for an additional 4 minutes, resulting in a total runtime of 10 minutes per injection. Mobile phase flow rate was held at 0.35 mL/min for the first 1.5 minutes, increased to 0.5 mL/min, and held for the final 4 minutes.

The high-resolution mass spectrometer was operated in full scan mode at 120,000 resolution and mass-to-charge ratio ($m/z$) range 85–1275. Probe temperature, capillary temperature, sweep gas, and S-Lens RF levels were maintained at 200°C, 300°C, 1 arbitrary units (AU), and 45 AU, respectively, for both polarities. Positive tune settings for sheath gas, auxiliary gas, sweep gas and spray voltage setting were 45 AU, 25 AU, and 3.5 kV, respectively. Raw data files were extracted and aligned using apLCMS[31] with modifications by xMSanalyzer.[32] Uniquely detected ions consisted of accurate mass $m/z$, retention time and ion abundance, referred to as $m/z$ features. Data filtering was performed to remove $m/z$ features with median coefficient of variation within technical replicates ≥75%. Additionally, only samples with Pearson correlation within technical replicates ≥0.7 were used for downstream analysis. Feature intensities for triplicates were median summarized with the requirement that at least two replicates had non-missing values. Batch-effect correction was performed using ComBat.[33]

**TABLE 1** Characteristics of the overall sample by the two groups, normal cognition and mild cognitive impairment (MCI)

| Characteristic | Overall (n = 185) | Normal cognition (n = 92) | Mild cognitive impairment (n = 93) | *P* value |
|---|---|---|---|---|
| **Age (years)** | | | | |
| Mean ± SD (N) | 64.4 ± 8.2 (185) | 62.7 ± 7.1 (92) | 66.1 ± 8.9 (93) | .0071 |
| **Sex** | | | | |
| Female | 116 (62.7) | 62 (67.4) | 54 (58.1) | .19 |
| Male | 69 (37.3) | 30 (32.6) | 39 (41.9) | |
| **Race** | | | | |
| White | 117 (63.2) | 63 (68.5) | 54 (58.1) | .24 |
| Black or African American | 65 (35.1) | 27 (29.3) | 38 (40.9) | |
| Other | 3 (1.6) | 2 (2.2) | 1 (1.1) | |
| **Education (years)** | | | | |
| Mean ± SD (N) | 16.3 ± 2.9 (179) | 16.6 ± 3.0 (92) | 15.9 ± 2.9 (87) | .23 |
| **Smoking status** | | | | |
| Never | 44 (37.9) | 32 (43.8) | 12 (27.9) | .0014 |
| Current | 21 (18.1) | 6 (8.2) | 15 (34.9) | |
| Past | 51 (44.0) | 35 (47.9) | 16 (37.2) | |
| **EtOH consumption** | | | | |
| Current | 88 (89.8) | 66 (93.0) | 22 (81.5) | .09 |
| Never or remote | 10 (10.2) | 5 (7.0) | 5 (18.5) | |
| **Body mass index (kg/m$^2$)** | | | | |
| Mean ± SD (N) | 27.3 ± 5.5 (178) | 27.4 ± 5.0 (92) | 27.3 ± 6.0 (86) | .66 |
| **Systolic blood pressure (mm Hg)** | | | | |
| Mean ± SD (N) | 128.9 ± 18.1 (179) | 129.6 ± 19.3 (92) | 128.1 ± 16.8 (87) | .80 |
| **Diastolic blood pressure (mm Hg)** | | | | |
| Mean ± SD (N) | 75.1 ± 12.4 (179) | 76.9 ± 12.1 (92) | 73.1 ± 12.5 (87) | .037 |
| **Pulse rate, beats per min** | | | | |
| Mean ± SD (N) | 67.8 ± 10.8 (179) | 66.9 ± 10.0 (92) | 68.8 ± 11.5 (87) | .30 |
| **Hypertension** | | | | |
| Yes | 79 (49.7) | 52 (57.8) | 27 (39.1) | .020 |
| No | 80 (50.3) | 38 (42.2) | 42 (60.9) | |
| **High cholesterol** | | | | |
| Yes | 70 (44.6) | 43 (48.9) | 27 (39.1) | .22 |
| No | 87 (55.4) | 45 (51.1) | 42 (60.9) | |
| **Diabetes mellitus** | | | | |
| Yes | 21 (13.1) | 11 (12.2) | 10 (14.3) | .70 |
| No | 139 (86.9) | 79 (87.8) | 60 (85.7) | |
| **Heart disease** | | | | |
| Yes | 13 (8.2) | 6 (6.7) | 7 (10.1) | .43 |
| No | 146 (91.8) | 84 (93.3) | 62 (89.9) | |
| **Congestive heart failure** | | | | |
| Yes | 4 (2.5) | 1 (1.1) | 3 (4.3) | .20 |
| No | 155 (97.5) | 89 (98.9) | 66 (95.7) | |
| **Depression** | | | | |
| Yes | 47 (29.4) | 20 (22.2) | 27 (38.6) | .024 |
| No | 113 (70.6) | 70 (77.8) | 43 (61.4) | |

(Continues)

**TABLE 1** (Continued)

| Characteristic | Overall (n = 185) | Normal cognition (n = 92) | Mild cognitive impairment (n = 93) | *P* value |
|---|---|---|---|---|
| **Atrial fibrillation or arrythmias** | | | | |
| Yes | 20 (12.7) | 11 (12.4) | 9 (13.2) | .87 |
| No | 137 (87.3) | 78 (87.6) | 59 (86.8) | |
| **MOCA, score** | | | | |
| Mean ± SD (N) | 24.3 ± 3.7 (162) | 26.6 ± 2.6 (92) | 21.3 ± 2.8 (70) | <.0001 |
| **HVLTR, delayed recall** | | | | |
| Mean ± SD (N) | 8.1 ± 3.2 (161) | 9.7 ± 2.0 (92) | 6.0 ± 3.4 (69) | <.0001 |
| **Trail Part A (seconds)** | | | | |
| Mean ± SD (N) | 39.3 ± 16.6 (162) | 34.9 ± 11.1 (92) | 45.1 ± 20.6 (70) | .0008 |
| **Trail Part B (seconds)** | | | | |
| Mean ± SD (N) | 108.8 ± 67.1 (161) | 83.3 ± 41.0 (92) | 142.8 ± 79.3 (69) | <.0001 |
| **Ab42 (pg./dl)** | | | | |
| Mean ± SD (N) | 255.5 ± 83.2 (183) | 256.0 ± 61.1 (91) | 255.1 ± 100.8 (92) | .61 |
| **tau (pg./dl)** | | | | |
| Mean ± SD (N) | 60.4 ± 35.8 (183) | 48.4 ± 20.6 (91) | 72.2 ± 43.2 (92) | <.0001 |
| **Ptau (pg/dl)** | | | | |
| Mean ± SD (N) | 15.7 ± 9.5 (180) | 12.3 ± 6.5 (90) | 19.0 ± 10.9 (90) | <.0001 |
| **Total hippocampal volume** | | | | |
| Mean ± SD (N) | 7303 ± 1046 (139) | 7654 ± 881.8 (80) | 6828 ± 1071 (59) | <.0001 |

Abbreviations: EtOH, ethyl alcohol; HVLTR, Hopkins Verbal Learning Test-Revised; MOCA, Montreal Cognitive Assessment; SD, standard deviation.

## 2.6 | Metabolome-wide association analysis

A feature was retained for further analysis if at least 90% of the subjects had non-zero intensity reading in either MCI or NC groups. After exclusion, the missing values for a feature were imputed as half of the lowest signal detected for that feature across all samples. After data filtering, all intensity values were $\log_2$ transformed to reduce heteroscedasticity and quantile normalized to reduce systematic errors due to technical and other non-biological factors. Metabolome-wide association analysis was conducted using partial least squares discriminant analysis (PLS-DA) implemented in the mixOmics[34] R package and features were selected based on the variable importance for projection (VIP) criteria. *P*-values were obtained for each feature using a permutation test. A 1000-permutation approach was performed by randomly shuffling the group labels of subjects and performing feature selection using PLS-DA at each iteration.[30] Multiple testing correction was performed using Storey and Tibshirani false discovery rate (FDR) adjustment.[35] Discriminatory features were selected using the thresholds of VIP ≥ 2, permutation derived $P < .05$, and FDR < 0.1. Only features that passed all three criteria were considered significantly different between the two groups. Manhattan plot was used to visualize the pattern of differential expression across all features with respect to retention time. Fold change of $\log_2$ transformed intensity values was calculated for each feature as the difference between the average intensity of the two groups, $\log_2 FC = average_{NC} - average_{MCI}$. Two-way hierarchical clustering analysis (HCA) was used to visualize the clustering pattern of discriminatory features and samples.

## 2.7 | Pathway analysis

Pathway enrichment analysis was performed using mummichog (v2.0.6), which uses both *m/z* and retention time, and included discriminatory features that met the following criteria: VIP ≥ 1.5, $P < .05$, and FDR <0.1. A lower VIP was used to increase enrichment within the pathway and prevent information loss.[10,36] Detailed descriptions of mummichog computational procedures were previously published for V1.0.[37] Discriminatory features detected in the pathways were further tested for differential expression between the NC and MCI groups using Wilcoxon rank sum test.

Additional pathway analyses were performed using Cystoscape-based metabolomic pathway analysis and visualization using Metscape.[38] MetScape is a plug-in for Cytoscape, an open source software platform for visualizing complex networks and provides a method to use experimental data leveraged with bioinformatic databases of metabolites, genes, and pathways to display them in the context of system networks. We used that tool to provide complementary information on possible metabolic differences between MCI and NC.

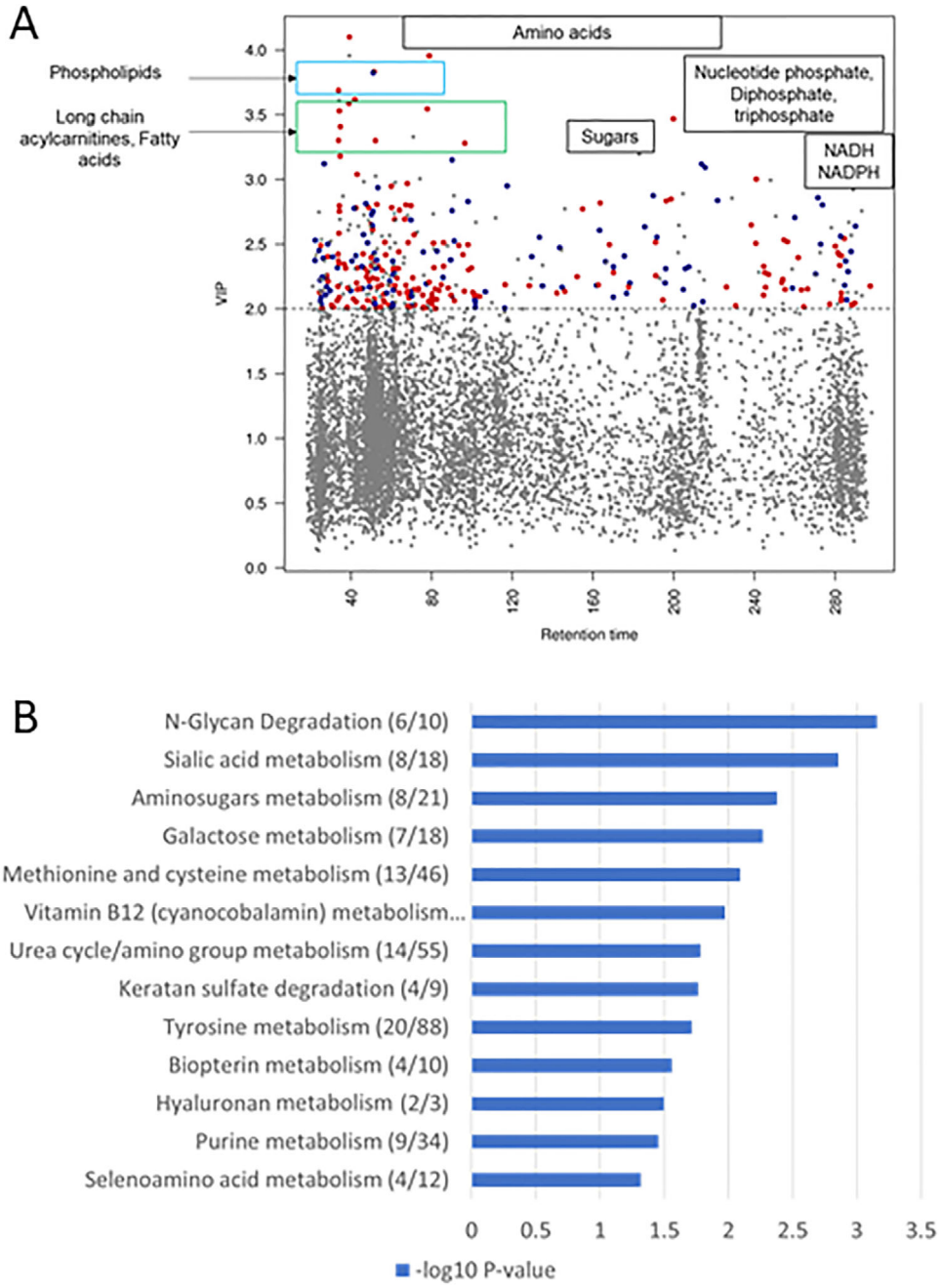


**FIGURE 1** A, Manhattan plot shows the variable importance for projection (VIP) and mass-to-charge ratio (*m/z*) of 8043 features. A total of 294 features were significantly different between mild cognitive impairment (MCI) cases (n = 93) and controls (n = 92) by partial least squares discriminant analysis (PLS-DA) using a VIP measure of 2.0 or greater (threshold indicated by horizontal line). One hundred eighty seven metabolic features increased (red dots) and 107 decreased (blue dots) in MCI patients compared to controls are indicated. Metabolite classes detected at different retention time segments are annotated in the boxes. B, Pathways altered in MCI compared to normal controls. Pathway analysis was performed using Mummichog 2.0.6 on the 1049 features identified by PLS-DA with a VIP ≥ 1.5

## 2.8 | Metabolite annotation and identification

Metabolite annotation and identification was performed using MS/MS, comparison with in-house library of confirmed metabolites, and using xMSannotator[33] with the Human Metabolome Database[34] (HMDB). Discriminatory features that were associated with the significantly enriched pathways and had $P < .05$ using the Wilcoxon rank sum test were selected for MS/MS analysis. For MS/MS, samples were analyzed using a Thermo Fusion Orbitrap high-resolution (120,000 mass resolution) mass spectrometer (Thermo Fisher Scientific, San Diego, CA) operated in positive ion mode with 5-minutes HILIC column chromatography and similar source conditions used for the untargeted metabolic profiling. Prior to analysis, CSF proteins were precipitated using acetonitrile:water (2:1 vol/vol) and allowed to sit on ice for 30

minutes. The supernatant was then carefully pipetted for MS/MS analysis. The tandem mass spectrometry data were processed using the *xcmsSet* and *xcmsFragments* functions in XCMS[39] to extract the MS/MS fragments associated with each parent mass and the experimental spectra were compared to in-silico fragmentation using MetFrag[40] or the spectra available from mzCloud (https://www.mzcloud.org/).

We further annotated and confirmed identities of the selected metabolites using an in-house library of metabolites that have been previously confirmed by comparing the retention time and MS/MS of the metabolic feature with authentic standards. Additionally, we performed computational annotation using xMSannotator[33] (v1.3.2) with the HMDB[34] (v3.5). xMSannotator uses adduct/isotope patterns, correlation in intensities across all samples, retention time difference between adducts/isotopes of a metabolite, and network and pathway associations for associating *m/z* features with known metabolites and categorizing database matches into different confidence levels.[41] This multi-step annotation process reduces the number of false matches compared to only *m/z*-based database search. Metabolite identification levels were assigned using an adapted version of the criteria proposed by Schymanski et al.: (1) confirmed by MS/MS and co-elution with authentic standards (level 1); (2) confirmed by MS/MS and matches with online databases or in-silico predicted spectra (level 2); (3) confirmed by MS/MS at the chemical class level, but no evidence for a specific metabolite (level 3); (4) computationally assigned annotation using xMSannotator (medium or high confidence) (level 4); (5) accurate mass match (level 5).[42]

### 2.9 | Association of discriminatory features with other disease phenotypes

Discriminatory metabolites associated with significantly enriched pathways were then tested for associations with three AD phenotypical or endophenotypic areas: cognitive performance (MoCA for global function, TMT A and B for executive function, and HVLT-delayed recall for episodic memory), neuroimaging (hippocampal volume and cortical thickness as indicators of neurodegeneration) and CSF AD biomarkers $A\beta_{1\text{-}42}$ and total and phosphorylated tau using Spearman's correlation analyses. A heatmap was used to visualize the correlation patterns between significant metabolic features and these measures.

## 3 | RESULTS

### 3.1 | Participants

Of the 185 participants who provided CSF, 93 were MCI and 92 were normal controls. The basic clinical characteristics of the sample are provided in Table 1. The MCI group were older ($P = .007$) and had higher levels of tau and p-tau (both $P < .0001$), but not $A\beta$ ($P = .6$).They also had lower cognitive performance in all measures as expected and lower hippocampal volume ($P < .0001$).

### 3.2 | MWAS results

Overall, 13,064 features were detected, and 8043 features met the data filtering criteria and were used for downstream analyses. Using PLS-DA, 294 discriminatory features were identified using the predefined criteria (Figure 1A). Of those, 107 features were underexpressed and 187 features were overexpressed in MCI patients relative to NC, as shown in Figure 1A. Two-way HCA using the 294 discriminatory features identified 19 clusters of samples indicating clinical and metabolic heterogeneity within the MCI group (Figure S2 in supporting information). Clusters 13, 9, and 15 (blue box) primarily comprised the MCI samples. Seventy clusters comprising features with similar abundance levels across samples were identified. Of the 294 features, 94 were successfully matched to known metabolites in HMDB using xMSannotator with an annotation confidence score of medium or high (Table S1 in supporting information).

### 3.3 | Pathway analysis

To enhance the coverage of metabolites for pathway enrichment analyses and to prevent information loss, 1049 discriminatory features were included using the less stringent criteria of VIP >1.5, $P < .05$, and FDR <0.1. We identified 13 pathways that were perturbed between the MCI and normal control groups, which are shown in Figure 1B. The top four pathways were related to bioenergetics and glucose metabolism: N-glycan ($P = .0007$), sialic acid ($P = .0014$), amino-sugars ($P = .0042$), and galactose ($P = .0054$) metabolism. Keratan sulfate ($P = .0173$), methionine ($P = .0081$), cyanocobalamin ($P = .0106$), tyrosine ($P = .0193$), purine ($P = .0352$) and biopterine ($P = .0275$) were also differentially activated between the two groups. Within the enriched pathways that were significantly different between NC and MCI, 15 features with an identification confidence of 1 to 5 were differentially expressed and are shown in Table 2. These features were then included in the Metscape analysis and visualization, leading to a signature that includes increased expressions of features related to sugar metabolism/bioenergetics, homocysteine, tyrosine and biopterin pathways, and lower expression of methionine. The final networks with relevant signature features are provided in Figure 2. The box plots for these 15 features are also provided in Figure 3. The complete list of features in these analyses is provided in Table S2 in supporting information.

### 3.4 | Correlation with disease phenotype

We then explored the associations between these signature features with disease phenotypes. These results are shown in Figure 4. Increased expression of bioenergetics and glucose metabolism were associated with higher tau and ptau but also with lower cognitive performance, hippocampal volume, and cortical thickness. Sugar metabolism dysregulations were associated with increased tau, and

**TABLE 2** Results of the pathway enrichment analysis with the significant features and associated pathways in the normal versus MCI groups

| *m/z* | time (s) | Feature name (KEGG compound name) | Pathway(s)[a] | Fold change[d] | VIP | Wilcoxon P | Metabolite identification level[c] | Adduct |
|---|---|---|---|---|---|---|---|---|
| 173.0434 | 52 | L-Ribulose (C00508)[b] | Tyrosine metabolism; Purine metabolism | −0.1642 | 3.30 | 0.0001 | 3 | M+Na[1+] |
| 205.0682 | 62 | D-Sorbitol (C00794 )[b] | Galactose metabolism | −0.124 | 1.97 | 0.0025 | 5 | M+Na[1+] |
| 365.1054 | 164 | Maltose (C00208 )[b] | Sialic acid metabolism; Galactose metabolism | −0.2469 | 2.81 | 0.0055 | 5 | M+Na[1+] |
| 385.1303 | 73 | S-Adenosylhomocysteine (C00021) | Methionine and cysteine metabolism; Vitamin B12 (cyanocobalamin) metabolism; Urea cycle/amino group metabolism; Tyrosine metabolism | −0.2034 | 2.15 | 0.0167 | 1 | M+H[1+] |
| 517.9829 | 81 | 7,8-Dihydroneopterin 3′-triphosphate (C04895)[b] | Biopterin metabolism | −0.6569 | 2.32 | 0.0217 | 5 | M+Na[1+] |
| 255.1076 | 68 | Galactosylglycerol (C05401) | Sialic acid metabolism; Galactose metabolism | −0.4977 | 2.72 | 0.0231 | 4 | M+H[1+] |
| 260.0538 | 57 | N-Acetyl-D-glucosamine 6-phosphate (C00357)[b] | Aminosugars metabolism | −0.1686 | 2.05 | 0.0248 | 5 | M+H[1+] |
| 223.0826 | 53 | Salsolinol 1-carboxylate (C06160) | Tyrosine metabolism | −0.374 | 2.22 | 0.0271 | 4 | M+H[1+] |
| 708.2568 | 255 | N-acetyl-alpha-D-glucosamine (C00043)[b] | N-Glycan degradation; Keratan sulfate degradation | −0.308 | 2.15 | 0.0289 | 4 | M+H[1+] |
| 399.1444 | 145 | S-Adenosylmethionine (C00019) | Methionine and cysteine metabolism; Vitamin B12 (cyanocobalamin) metabolism; Urea cycle/amino group metabolism; Tyrosine metabolism | 0.3296 | 2.17 | 0.0334 | 1 | M+H[1+] |
| 384.1499 | 231 | beta-D-Galactosyl-1,4-N-acetyl-D-glucosamine (C00611)[b] | N-Glycan Degradation; Aminosugars metabolism; Galactose metabolism | −0.1902 | 2.02 | 0.0357 | 5 | M+H[1+] |
| 221.042 | 61 | Vanillylmandelic acid (C05584) | Tyrosine metabolism | −0.5378 | 1.92 | 0.0365 | 4 | M+Na[1+] |
| 799.6688 | 37 | Levothyroxine (C01829) | Tyrosine metabolism | −0.7153 | 2.31 | 0.0416 | 4 | M+Na[1+] |
| 277.0894 | 67 | 3-beta-D-Galactosyl-sn-glycerol (C03692)[b] | Sialic acid metabolism; Galactose metabolism | −0.1336 | 2.18 | 0.0474 | 4 | M+Na[1+] |
| 244.0797 | 49 | GlcNAc (C00140)[b] | N-Glycan degradation; Sialic acid metabolism; Aminosugars metabolism; Galactose metabolism; Keratan sulfate degradation; Hyaluronan Metabolism | −0.0803 | 2.22 | 0.0507 | 5 | M+Na[1+] |

[a]Some compounds were matched or involved in multiple pathways.
[b]These features had multiple chemical names or were matched to multiple metabolites in the databases (we report the KEGG compound name involved in the significant pathway).
[c]Description of metabolite identification levels (adapted from Schymanski et al.[42]):
Level 1: confirmed by MS/MS and co-elution with authentic standards
Level 2: confirmed by MS/MS and matches with online databases or in-silico predicted spectra
Level 3: confirmed by MS/MS at the chemical class level, but no evidence for a specific metabolite
Level 4: computationally assigned annotation using xMSannotator (medium or high confidence)
Level 5: accurate mass match
[d](log2; NC vs MCI) -ve: lower in NC +ve: higher in NC.
Abbreviations: KEGG, Kyoto Encyclopedia of Genes and Genomes; MCI, mild cognitive impairment; MS/MS, tandem mass spectrometry; *m/z*, mass-to-charge ratio; NC, normal control; VIP, variable importance for projection

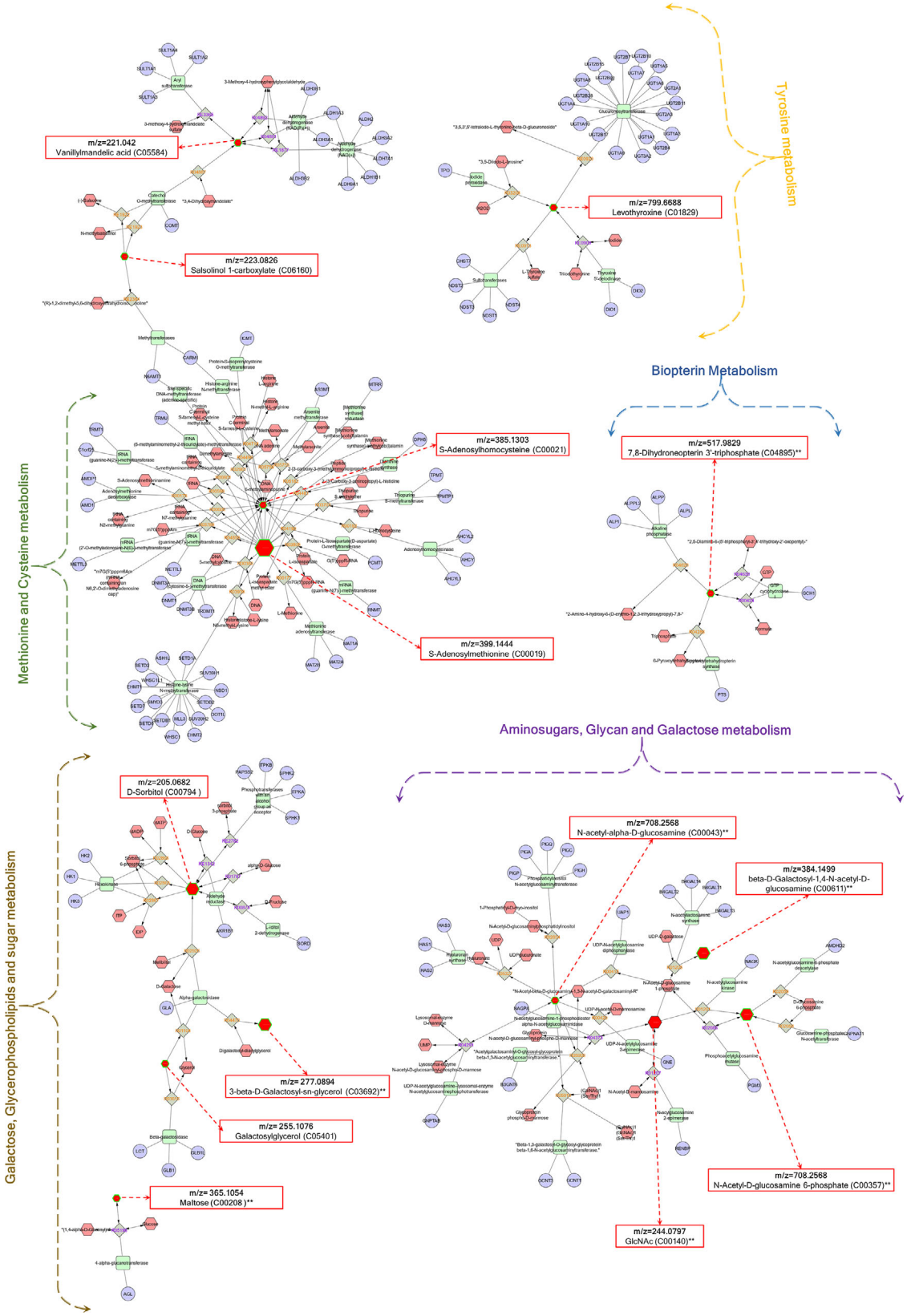


**FIGURE 2** Overall metabolomic networks and related features comprising the metabolomic signature in the cerebrospinal fluid of individuals with mild cognitive impairment (MCI). The image was obtained using Metscape Plug-in for Cytoscape using the 15 features included in the MCI signature along with the fold change and *P*-value and the Compound-Reaction-Enzyme-Gene option selected. The Network is then built from the underlying data by finding compounds that participate in reactions that are catalyzed by enzymes that are encoded by genes

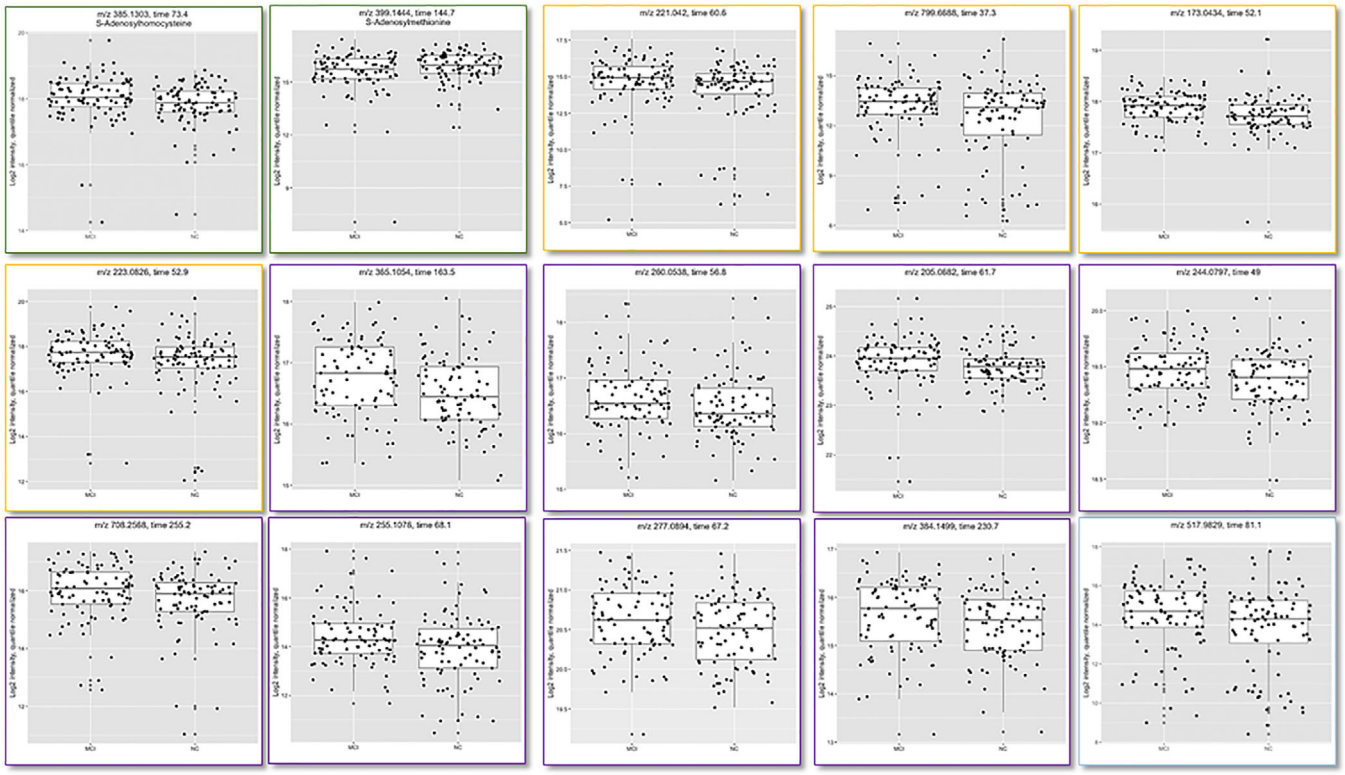


**FIGURE 3** Box plots for the 15 differentially expressed features identified in the cerebrospinal fluid of individuals with mild cognitive impairment. Green box plots are in the methionine pathway, brown in the sugar metabolism pathways, purple in the tyrosine metabolism pathway, and blue in the biopterin pathway

ptau. Further, 5 of these features were associated with decreased cortical thickness; hippocampal volume; and cognitive performance on MoCA, TMT, and delayed recall. S-adenosylhomocysteine (SAH) was associated with lower MoCA scores and decreased cortical thickness. In the tyrosine pathway, salsolinol-1-carboxylate was associated with higher tau and ptau whereas Vanillylmandelic acid (VMA) was associated with lower MoCA score. Finally, features in the biopterin pathway were not associated with any disease phenotype. Detailed results are provided in Table S3 in supporting information. Correlation with demographics are also provided in Table S4 in supporting information.

## 4 | DISCUSSION

This study of untargeted HRM identified a CSF signature of amnestic MCI characterized by dysregulation of multiple pathways including sugar, homocysteine/methionine, and tyrosine metabolism. Multiple features within this signature were associated with increased total tau and ptau biomarkers and lower scores on cognitive measures, hippocampal volume, and cortical thickness.

Although targeted metabolomic approaches have been used in multiple tissues and samples such as Biocrates AbsoluteIDQ-p180 kit,[43] untargeted metabolomics in the CSF have been less common. The latter can be complementary to prior targeted platforms and plasma analyses and may identify new markers or new potential therapeutic targets in AD. The recent advance in MS technology and related bioinformatics have enhanced the potential for the application of metabolomics in AD.[44] Indeed, over the last decade reports using untargeted metabolomics have suggested a significant previously unrecognized metabolic derangement in AD *post mortem* brains, plasma, and to a lesser extent CSF.[45,46] Our study adds to these reports by confirming and expanding on previously described impaired pathways or identifying new ones. We discuss these in the next sections.

Multiple studies have suggested an association between AD and impaired glucose metabolism that may be pronounced in those with type 2 diabetes and insulin resistance.[47,48] Prior fluorodeoxyglucose-positron emission tomography (FDG-PET) scans have suggested decreased brain metabolism across the spectrum of AD.[49,50] Our study suggests that in the CSF of those with MCI, there was evidence for dysregulation of multiple glucose metabolism pathways and related increase in glucose metabolism byproducts. Taken together, the increase in CSF features of sugar metabolism pathways coupled with the previously reported brain hypometabolism may in part be explained by a lower brain glucose uptake, for example, secondary to glucose uptake transporter impairment,[51,52] leading to increased CSF levels. An alternative explanation is that the possible central insulin resistance reported in AD is associated with increases in metabolic by-products in the brain and CSF. This is further supported by our observation that these increased metabolic features are associated with greater tau measures and with lower performance on cognitive

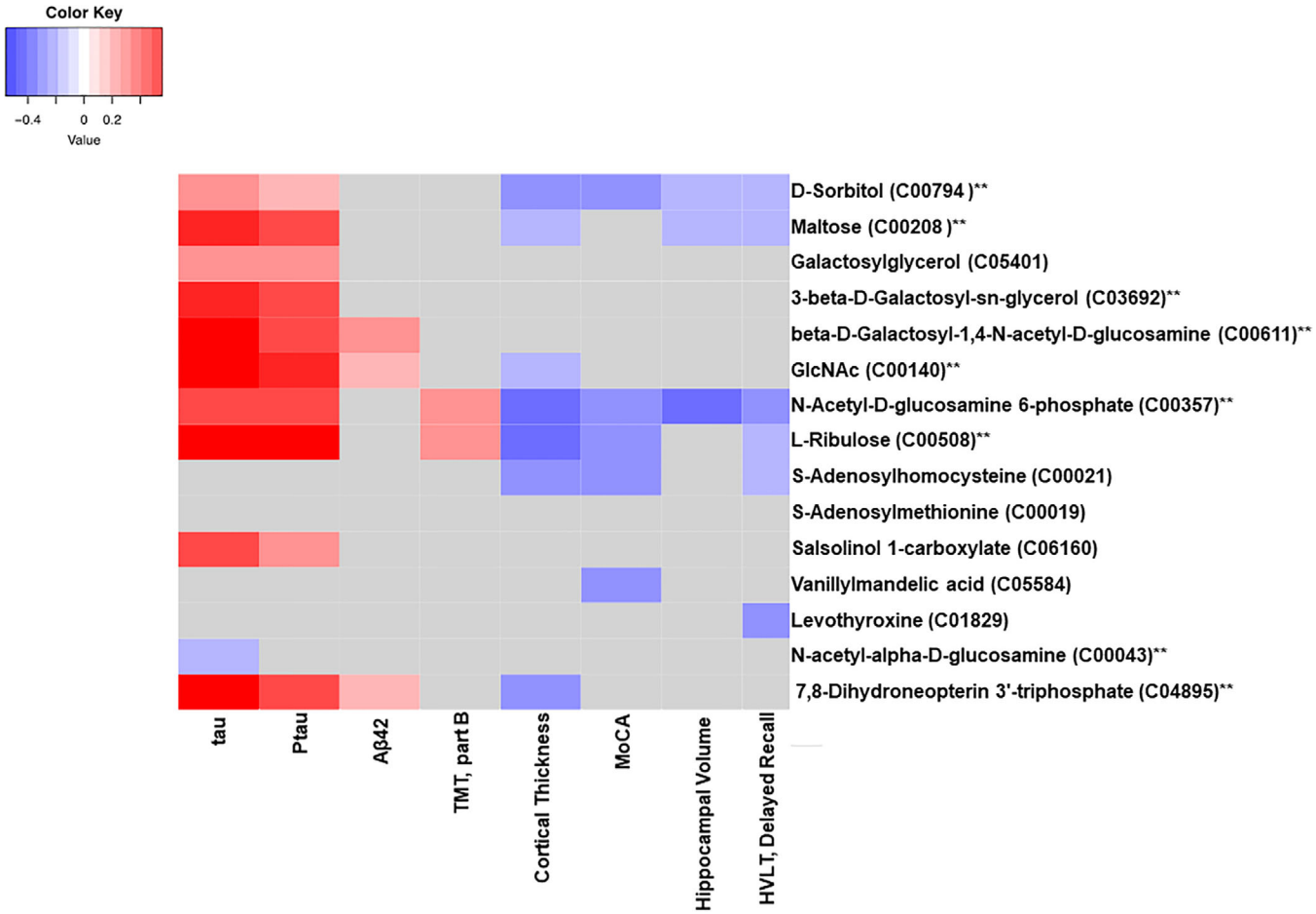


**FIGURE 4** Correlations between significant features and disease phenotypes. Spearman correlation coefficients. Red indicates positive correlations and blue indicates negative correlations. Correlations with $P \geq 0.05$ are marked in gray. **These Features had multiple chemical names or were matched to multiple metabolites in the databases (we report the KEGG compound name involved in the significant pathway)

assessments, hippocampal volume, and cortical thickness. Taken together, our finding may offer support for multiple sugar metabolism pathways as therapeutic targets in AD.

Our observation that alterations in pathways related to methionine and homocysteine metabolism is of great interest. Specifically, S-adenosylmethionine (SAM) was underexpressed and SAH was overexpressed in CSF of the MCI participants. SAM is a key molecule in the methionine cycle involved in nucleic acid and protein metabolism and synthesis. SAH is formed by demethylation of SAM. Prior reports suggest that SAM is decreased and SAH is increased in CSF of AD and related to tau biomarkers.[53] However, in this study only SAM was related to additional disease phenotypes including cognitive measures and cortical thickness. Nevertheless, this untargeted approach suggests that homocysteine-methionine pathways are dysregulated in the prodromal stages of AD.

We identified perturbations in tyrosine pathways with overlapping features in the purine, methionine, and homocysteine pathways, including SAM, SAH, VMA, and thyroxine. These cycles are involved in catecholamine and serotonin neurotransmitter systems and might be altered in AD.[54] A prior CSF analysis in a smaller number of MCI using a targeted metabolomic approach suggested a similar finding of impairments in methionine and tyrosine pathways.[55] Despite the difference between the groups in this pathway, there were minimal associations with the other disease measures.

There are multiple advantages to this study including the untargeted and advanced bioinformatic approaches, which allowed us to consider many pathways and features, the comparably larger number of samples with CSF, and the availability of multiple additional disease phenotypes that offer greater confidence in the associations with MCI.

The limitations include the cross-sectional design and the number of identified features that could not be matched to known metabolites or matched to multiple metabolites, which is a major bottleneck in untargeted metabolomics.[6] Even with identified metabolites, the certainty of feature identity is another limitation to untargeted metabolomic approaches. We used MS/MS with an in-house library of confirmed metabolites in the Clinical Biomarker Lab where these analyses were performed using authentic standards to confirm these identities and we provide a standard scale of confidence in all our results. This coupled with advanced bioinformatics tools for metabolite identification and annotation enhanced the reliability of the identity of our metabolites compared to many prior untargeted studies.

Clinical translations of these findings are important. The key pathways that are perturbed in AD are potential targets for existing or new drug developments. For example, insulin and other antidiabetic agents may address the sugar metabolism abnormalities identified in this analysis.[56,57] Drugs that may restore balance between SAM and SAH or enhance tyrosine metabolism may also be of relevance in drug development of AD.[58]

## 5 | CONCLUSION

In this untargeted metabolomic study of CSF, we identified a metabolic signature characterized by impairments in sugar metabolism and methionine, homocysteine, and tyrosine pathways in MCI. These offer insight into the metabolic alterations that occur in predementia stages of AD and offer potential therapeutic targets.

### ACKNOWLEDGMENTS

This work was supported by the National Institutes of Health (Grants number RF1AG051633, RF1AG057470, R01AG049752, R01AG042127). Authors would like to thank Ken Liu, PhD (Emory University) for his help with the MS/MS analysis and the B-SHARP participants for their valuable contribution to this research.

### CONFLICTS OF INTEREST

The authors have no competing interests to declare.

### REFERENCES

1. Talwar P, Sinha J, Grover S, et al. Dissecting complex and multifactorial nature of Alzheimer's disease pathogenesis: a clinical, genomic, and systems biology perspective. *Mol Neurobiol*. 2016;53:4833-4864.
2. Rollo JL, Banihashemi N, Vafaee F, Crawford JW, Kuncic Z, Holsinger RM. Unraveling the mechanistic complexity of Alzheimer's disease through systems biology. *Alzheimers Dement*. 2016;12:708-718.
3. Alkadhi K, Eriksen J. The complex and multifactorial nature of Alzheimer's disease. *Curr Neuropharmacol*. 2011;9:586.
4. Carreiras MC, Mendes E, Perry MJ, Francisco AP, Marco-Contelles J. The multifactorial nature of Alzheimer's disease for developing potential therapeutics. *Curr Top Med Chem*. 2013;13:1745-1770.
5. Wang M, Roussos P, McKenzie A, et al. Integrative network analysis of nineteen brain regions identifies molecular signatures and networks underlying selective regional vulnerability to Alzheimer's disease. *Genome Med*. 2016;8:104.
6. Uppal K, Walker DI, Liu K, Li S, Go YM, Jones DP. Computational metabolomics: a framework for the million metabolome. *Chem Res Toxicol*. 2016;29:1956-1975.
7. Uppal K, Salinas JL, Monteiro WM, et al. Plasma metabolomics reveals membrane lipids, aspartate/asparagine and nucleotide metabolism pathway differences associated with chloroquine resistance in Plasmodium vivax malaria. *PLoS One*. 2017;12:e0182819.
8. Chandler JD, Hu X, Ko EJ, et al. Metabolic pathways of lung inflammation revealed by high-resolution metabolomics (HRM) of H1N1 influenza virus infection in mice. *Am J Physiol Regul Integr Comp Physiol*. 2016;311:R906-R16.
9. Frediani JK, Jones DP, Tukvadze N, et al. Plasma metabolomics in human pulmonary tuberculosis disease: a pilot study. *PLoS One*. 2014;9:e108854.
10. Sumarriva K, Uppal K, Ma C, et al. Arginine and carnitine metabolites are altered in diabetic retinopathy. *Invest Ophthalmol Vis Sci*. 2019;60:3119-3126.
11. Wishart DS, Feunang YD, Marcu A, et al. HMDB 4.0: the Human Metabolome Database for 2018. *Nucleic Acids Res*. 2018;46:D608-D617.
12. Patti GJ, Yanes O, Siuzdak G. Metabolomics: the apogee of the omics trilogy. *Nat Rev Mol Cell Biol*. 2012;13:263-269.
13. Mosconi L, Pupi A, De Leon MJ. Brain glucose hypometabolism and oxidative stress in preclinical Alzheimer's disease. *Ann N Y Acad Sci*. 2008;1147:180-195.
14. Kaddurah-Daouk R, Zhu H, Sharma S, et al. Alterations in metabolic pathways and networks in Alzheimer's disease. *Transl Psychiatry*. 2013;3:e244-e.
15. Trushina E, Dutta T, Persson X-MT, Mielke MM, Petersen RC. Identification of altered metabolic pathways in plasma and CSF in mild cognitive impairment and Alzheimer's disease using metabolomics. *PloS one*. 2013;8:e63644-e.
16. Ibáñez C, Simó C, Barupal DK, et al. A new metabolomic workflow for early detection of Alzheimer's disease. *J Chromatogr A*. 2013;1302:65-71.
17. Trushina E, Dutta T, Persson XM, Mielke MM, Petersen RC. Identification of altered metabolic pathways in plasma and CSF in mild cognitive impairment and Alzheimer's disease using metabolomics. *PLoS One*. 2013;8:e63644.
18. Motsinger-Reif AA, Zhu H, Kling MA, et al. Comparing metabolomic and pathologic biomarkers alone and in combination for discriminating Alzheimer's disease from normal cognitive aging. *Acta Neuropathol Commun*. 2013;1:28.
19. Niedzwiecki MM, Walker DI, Howell JC, et al. High-resolution metabolomic profiling of Alzheimer's disease in plasma. *Ann Clin Transl Neurol*. 2020;7:36-45.
20. Nasreddine ZS, Phillips NA, Bedirian V, et al. The Montreal Cognitive Assessment, MoCA: a brief screening tool for mild cognitive impairment. *J Am Geriatr Soc*. 2005;53:695-699.
21. Folstein MF, Folstein SE, McHugh PR. "Mini-mental state". A practical method for grading the cognitive state of patients for the clinician. *J Psychiatr Res*. 1975;12:189-198.
22. Hughes CP, Berg L, Danziger WL, Coben LA, Martin RL. A new clinical scale for the staging of dementia. *Br J Psychiatry*. 1982;140:566-572.
23. Wechsler D. *WMS-R : Wechsler Memory Scale–Revised : manual*. San Antonio: Psychological Corp.: Harcourt Brace Jovanovich; 1987.
24. Pfeffer RI, Kurosaki TT, Harrah CH, Jr., Chance JM, Filos S. Measurement of functional activities in older adults in the community. *J Gerontol*. 1982;37:323-329.
25. Petersen RC, Lopez O, Armstrong MJ, et al. Practice guideline update summary: mild cognitive impairment: Report of the Guideline Development, Dissemination, and Implementation Subcommittee of the American Academy of Neurology. *Neurology*. 2018;90:126-135.
26. Shaw LM, Vanderstichele H, Knapik-Czajka M, et al. Qualification of the analytical and clinical performance of CSF biomarker analyses in ADNI. *Acta Neuropathol*. 2011;121:597-609.
27. Schmidt MF, Storrs JM, Freeman KB, et al. A comparison of manual tracing and FreeSurfer for estimating hippocampal volume over the adult lifespan. *Hum Brain Mapp*. 2018;39:2500-2513.
28. Jack CR, Jr., Bennett DA, Blennow K, et al. NIA-AA research framework: toward a biological definition of Alzheimer's disease. *Alzheimers Dement*. 2018;14:535-652.
29. Accardi CJ, Walker DI, Uppal K, et al. High-resolution metabolomics for nutrition and health assessment of armed forces personnel. *J Occup Environ Med*. 2016;58:S80-S88.
30. Liu KH, Walker DI, Uppal K, et al. High-resolution metabolomics assessment of military personnel: evaluating analytical strategies for chemical detection. *J Occup Environ Med*. 2016;58:S53-S61.

31. Yu T, Park Y, Li S, Jones DP. Hybrid feature detection and information accumulation using high-resolution LC-MS metabolomics data. *J Proteome Res*. 2013;12:1419-1427.
32. Uppal K, Soltow QA, Strobel FH, et al. xMSanalyzer: automated pipeline for improved feature detection and downstream analysis of large-scale, non-targeted metabolomics data. *BMC Bioinformatics*. 2013;14:15.
33. Johnson WE, Li C, Rabinovic A. Adjusting batch effects in microarray expression data using empirical Bayes methods. *Biostatistics*. 2007;8:118-127.
34. Rohart F, Gautier B, Singh A, Le Cao KA. mixOmics: an R package for 'omics feature selection and multiple data integration. *PLoS Comput Biol*. 2017;13:e1005752.
35. Storey JD, Tibshirani R. Statistical significance for genomewide studies. *Proc. Natl. Acad. Sci.*. 2003;100:9440-9445.
36. Khatri P, Sirota M, Butte AJ. Ten years of pathway analysis: current approaches and outstanding challenges. *PLoS Comput Biol*. 2012;8:e1002375.
37. Li S, Park Y, Duraisingham S, et al. Predicting network activity from high throughput metabolomics. *PLoS Comput Biol*. 2013;9:e1003123.
38. Karnovsky A, Weymouth T, Hull T, et al. Metscape 2 bioinformatics tool for the analysis and visualization of metabolomics and gene expression data. *Bioinformatics*. 2012;28:373-380.
39. Smith CA, Want EJ, O'Maille G, Abagyan R, Siuzdak G. XCMS: processing mass spectrometry data for metabolite profiling using nonlinear peak alignment, matching, and identification. *Anal Chem*. 2006;78:779-787.
40. Ruttkies C, Schymanski EL, Wolf S, Hollender J, Neumann S. MetFrag relaunched: incorporating strategies beyond in silico fragmentation. *J Cheminform*. 2016;8:3.
41. Uppal K, Walker DI, Jones DP. xMSannotator: an r package for network-based annotation of high-resolution metabolomics data. *Anal Chem*. 2017;89:1063-1067.
42. Schymanski EL, Jeon J, Gulde R, et al. Identifying small molecules via high resolution mass spectrometry: communicating confidence. *Environ Sci Technol*. 2014;48:2097-2098.
43. Toledo JB, Arnold M, Kastenmüller G, et al. Metabolic network failures in Alzheimer's disease: a biochemical road map. *Alzheimers Dement*. 2017;13:965-984.
44. Wilkins JM, Trushina E. Application of metabolomics in Alzheimer's disease. *Front Neurol*. 2018;8:719.
45. Paglia G, Stocchero M, Cacciatore S, et al. Unbiased metabolomic investigation of Alzheimer's disease brain points to dysregulation of mitochondrial aspartate metabolism. *J Proteome Res*. 2016;15:608-618.
46. Graham SF, Chevallier OP, Elliott CT, et al. Untargeted metabolomic analysis of human plasma indicates differentially affected polyamine and L-arginine metabolism in mild cognitive impairment subjects converting to Alzheimer's disease. *PloS one*. 2015;10:e0119452-e.
47. Liu X, Wang W, Chen HL, Zhang HY, Zhang NX. Interplay between Alzheimer's disease and global glucose metabolism revealed by the metabolic profile alterations of pancreatic tissue and serum in APP/PS1 transgenic mice. *Acta Pharmacol Sin*. 2019;40:1259-1268.
48. Calsolaro V, Edison P. Alterations in Glucose metabolism in Alzheimer's disease. *Recent Pat Endocr Metab Immune Drug Discov*. 2016;10:31-39.
49. Mosconi L, Mistur R, Switalski R, et al. FDG-PET changes in brain glucose metabolism from normal cognition to pathologically verified Alzheimer's disease. *Eur J Nucl Med Mol Imaging*. 2009;36:811-822.
50. Haense C, Herholz K, Jagust WJ, Heiss WD. Performance of FDG PET for detection of Alzheimer's disease in two independent multicentre samples (NEST-DD and ADNI). *Dement Geriatr Cogn Disord*. 2009;28:259-266.
51. Pearson-Leary J, McNay EC. Novel Roles for the Insulin-Regulated Glucose Transporter-4 in Hippocampally Dependent Memory. *J Neurosci*. 2016;36:11851-1164.
52. Harr SD, Simonian NA, Hyman BT. Functional alterations in Alzheimer's disease: decreased glucose transporter 3 immunoreactivity in the perforant pathway terminal zone. *J Neuropathol Exp Neurol*. 1995;54:38-41.
53. Linnebank M, Popp J, Smulders Y, et al. S-adenosylmethionine is decreased in the cerebrospinal fluid of patients with Alzheimer's disease. *Neurodegener Dis*. 2010;7:373-378.
54. Trillo L, Das D, Hsieh W, et al. Ascending monoaminergic systems alterations in Alzheimer's disease. translating basic science into clinical care. *Neurosci Biobehav Rev*. 2013;37:1363-1379.
55. Kaddurah-Daouk R, Zhu H, Sharma S, et al. Alterations in metabolic pathways and networks in Alzheimer's disease. *Translational psychiatry*. 2013;3:e244-e.
56. Neth BJ, Craft S. Insulin resistance and Alzheimer's disease: bioenergetic linkages. *Front Aging Neurosci*. 2017;9:345.
57. Claxton A, Baker LD, Hanson A, et al. Long acting intranasal insulin detemir improves cognition for adults with mild cognitive impairment or early-stage Alzheimer's disease dementia. *J Alzheimers Dis*. 2015;45:1269-1270.
58. Chen H, Liu S, Ji L, et al. Folic acid supplementation mitigates Alzheimer's disease by reducing inflammation: a randomized controlled trial. *Mediators Inflamm*. 2016;2016:5912146.

## SUPPORTING INFORMATION

Additional supporting information may be found online in the Supporting Information section at the end of the article.

**How to cite this article:** Hajjar I, Liu C, Jones DP, Uppal K. Untargeted metabolomics reveal dysregulations in sugar, methionine, and tyrosine pathways in the prodromal state of AD. *Alzheimer's Dement*. 2020;12:e12064.
https://doi.org/10.1002/dad2.12064